PHILOSOPHICAL TRANSACTIONS OF THE ROYAL SOCIETY A MATHEMATICAL, PHYSICAL & ENGINEERING SCIENCES

Coherent v.l.f. Waves in the Magnetosphere [and Discussion]

R. A. Helliwell and K. Bullough

Phil. Trans. R. Soc. Lond. A 1975 **280**, 137-149
doi: 10.1098/rsta.1975.0097

Phil. Trans. R. Soc. Lond. A. **280**, 137–149 (1975) [137]
Printed in Great Britain

Coherent v.l.f. waves in the magnetosphere

By R. A. Helliwell
Radioscience Laboratory, Stanford University, Stanford, California, U.S.A.

[Plates 3–6]

V.l.f. whistler-mode waves in the magnetosphere may be generated by natural lightning and v.l.f. transmitters, or through resonant interactions with radiation belt electrons. Such v.l.f. waves provide information on the hot and cold components of the magnetospheric plasma. Energetic electrons precipitated by whistler-mode waves may generate Bremsstrahlung X-rays and enhance the electron density of the ionosphere. Coherent signals transmitted from the ground can be amplified up to 30 dB in the magnetosphere; the amplified signal may trigger discrete v.l.f. emissions of both rising and falling frequency. V.l.f. line radiation from the magnetosphere is observed, apparently controlled by power line harmonic radiation from the ground. Triggered emission can be explained by using a new principle in which waves and cyclotron-resonant electrons interchange energy through a feedback process. Applications of controlled wave injection include: (1) diagnostic study of the magnetosphere; (2) plasma physics experiments; (3) controlled precipitation; and (4) v.l.f. communications.

1. Introduction

One of the fascinating topics in physics is non-thermal radiation of natural origin. Cherenkov and synchrotron radiation are examples. Sources include the Sun, the Earth, Jupiter and astrophysical bodies outside the Solar System. An especially remarkable class is the v.l.f. whistler-mode radiation from the Earth's magnetosphere. One type originates in an atmospheric lightning impulse which is spread out into a 'whistler' as it travels through the magnetosphere. Certain other types, such as chorus and hiss, originate within the magnetosphere through interaction with energetic particles of the Earth's radiation belts.

A comparison of the power spectral densities of various kinds of natural noise as observed near the Earth is given in figure 1. Except for synchrotron radiation, all types of Earth noise, including chorus and associated hiss, auroral hiss, highpass noise (also called kilometric radiation) and plasma waves, exceed all other types in intensity. Not only are the Earth noises non-thermal but some are remarkably coherent. The main purpose of this paper is to call attention to the properties of the narrow band discrete forms of noise known as chorus and triggered v.l.f. emissions. Because of their high intensity these signals are of interest in the study of processes for generating strong coherent radiation in natural and laboratory plasmas. They also cause significant precipitation of particles from the radiation belts.

The origin of this subject is as remarkable as the properties of the waves themselves. The starting point was the whistler, accidently discovered by the German scientist Barkhausen (1919) while he was listening in on enemy telephone conversations at the front lines during World War I. He reported his results in *Nature* in 1919 but could not explain them. The mystery was partially resolved shortly after the magnetoionic theory was introduced. Using this theory, Eckersley (1935) showed how a lightning impulse could be transformed, by the ionosphere, into a descending tone. His calculation required that the Lorentz polarization term be omitted from the magnetoionic theory. What Eckersley could not explain however was the long duration

(up to several seconds) of this dispersed signal, requiring an extremely long path of propagation through the ionosphere.

The path travelled by the whistler remained unknown until Storey (1953) performed his imaginative experiments in 1951. He showed that the whistler energy was guided by the Earth's field along paths extending to altitudes of several Earth radii. A sketch of the mechanism, modified to include ducting, is shown in figure 2. It was the whistler and its strange path requirement that in fact revealed the presence of the magnetosphere itself. The whistler required a relatively high equatorial electron density, estimated by Storey at about 600 e/cm^3. During preparation for the International Geophysical Year (1957) further properties of whistlers were discovered including the whistler 'nose' and ducting (Helliwell 1965). These features enabled whistlers to be used for mapping the density of electrons in the magnetosphere (Park 1972).

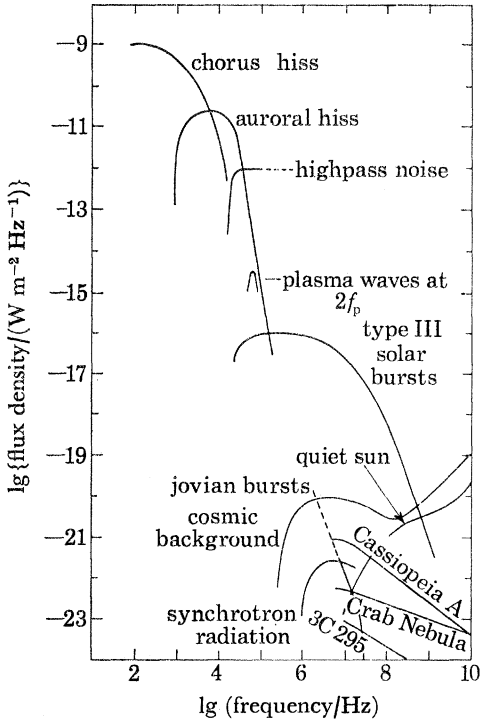

FIGURE 1. Flux densities of emissions detected by OGO's 1 and 3 compared to those from other sources. Levels given are those of strong events measured by satellites, or, in the case of extra-terrestrial sources, measured at 1 AU (after Dunckel 1974).

Because of the success of Eckersley and Storey in applying the magnetoionic theory to the interpretation of whistlers, they remained the main object of study for some years. However, the early observations of natural v.l.f. waves had revealed a remarkable variety of odd noises, including chorus, variable tones and hiss (Burton & Boardman 1933). As the whistler itself became established as a measurement tool, attention was focused on the nature of the natural noise coming from the magnetosphere. This is the main topic of the present paper.

Following a brief review of v.l.f. wave phenomena a suggested model of electron-wave interaction in the magnetosphere will be outlined. The results of a series of controlled v.l.f. wave injection experiments are then described. The paper concludes with a summary of what we know and an outline of present and future application of v.l.f. waves in the magnetosphere.

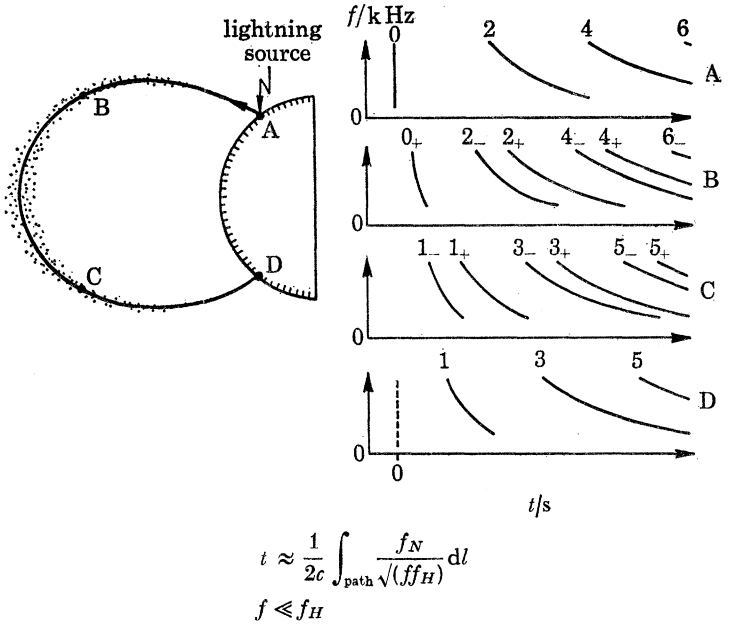

$$t \approx \frac{1}{2c}\int_{\text{path}} \frac{f_N}{\sqrt{(f f_H)}}\,\mathrm{d}l$$

$$f \ll f_H$$

FIGURE 2. Echoing ducted whistlers are observed on the ground at points A and D and in satellites at points B and C. The lightning source is located at point A, and the Eckersley approximation is used to sketch the spectra. The vertical dashed line in the lowest spectrogram represents the attenuated sferic arriving at D via the Earth–ionosphere waveguide (figure 1, Helliwell 1969).

2. THE PHENOMENA

Whistler propagation was illustrated in figure 2 for the purpose of indicating the elementary features of dispersion and guidance. Experiments conducted after Storey's initial work revealed a number of new features. It was found for example that whistlers observed on the ground usually travel in ducts, as sketched in figure 3 (Smith, Helliwell & Yabroff 1960). These ducts are believed to consist of field aligned enhancements of electron density. A whistler entering such an irregularity is guided in much the same way that light rays are guided in an optical fibre. Many such field-alined irregularities may be present in the magnetosphere at any one time. In the sketch of figure 3 only two ducts are shown. The spectra of the whistlers in these two ducts as recorded on the ground are shown in the accompanying spectrogram. A satellite at position S records leakage from the outer duct when the frequency of the wave exceeds one-half the local electron gyrofrequency, as shown in the sketch. Both ducting and leakage have been confirmed through satellite observations (Angerami 1970) and are explained by the magnetoionic theory using electrons only.

Actual multipath nose whistlers are shown in spectrographic form in figure 4, plate 3. The top record shows many components (each parabolic in shape) excited by a single lightning flash. Each trace corresponds to a different geomagnetic latitude, which is measured by the frequency at the point on the trace of minimum delay, called the 'nose'. From the travel times at the noses corresponding values of the equatorial electron density are derived, giving a model of the magnetosphere (Carpenter & Park 1973). Changes in the nose frequency of a particular whistler are used to measure the north–south component of the drift of the duct (Carpenter Stone, Siren & Crystal 1972). This drift in turn yields the corresponding east–west component of electric field in the magnetosphere.

Unducted as well as ducted whistlers are observed with satellites and rockets. The mechanism of unducted propagation from a ground source to a satellite is sketched in figure 5. Three separate paths are shown. With the exception of the direct path, each path includes internal magnetospheric reflexions. This is an effect of protons, that cause the refractive index surface to close at frequencies below the lower hybrid resonance frequency (l.h.r.). A sketch of the reflexion mechanism, shown in parts (*c*) and (*d*) of figure 5, indicates the large angle between the direction of energy flow and the direction of the wave normal. Additional ion effects are observed at lower frequencies and at lower altitudes where helium and oxygen ions are important. Strong whistler dispersion is observed at both the proton (Gurnett, Skawhan, Smith & Brice 1965) and helium (Barrington & McEwen 1966) ion gyrofrequencies. In addition other

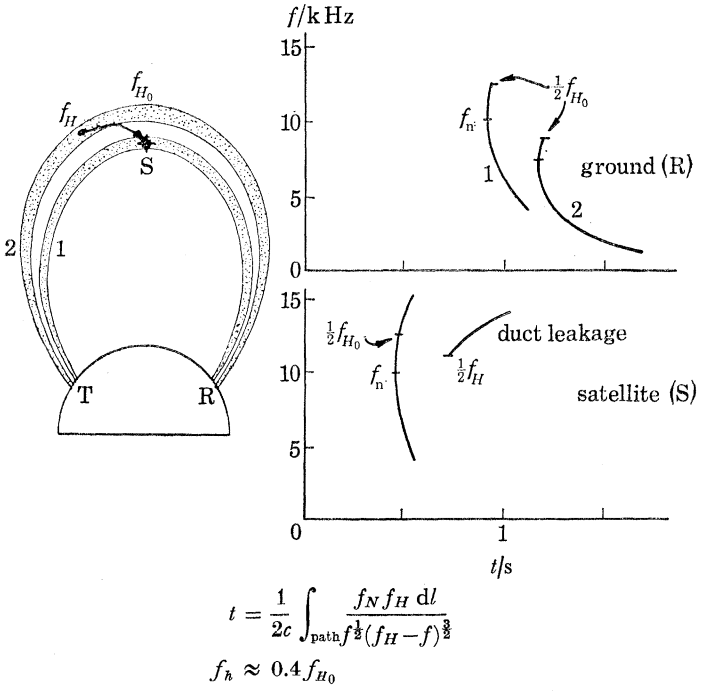

FIGURE 3. Multipath ducted nose whistlers observed on ground; leakage from ducts observed on satellite for $f > \frac{1}{2}f_H$. Nose frequency f_n gives path latitude; nose delay t_n gives electron concentration. f_H, electron gyrofrequency; f_N, electron plasma frequency, dl, element of path (figure 2, Helliwell 1969).

DESCRIPTION OF PLATE 3

FIGURE 4. Triggered emissions: upper panel shows multipath nose whistler and rising tones triggered by NAA at 14.7 kHz; lower panel shows discrete emissions triggered by nose whistlers at their upper cutoff frequencies ($\frac{1}{2}f_{H_0}$), Eights Station, 6 June 1963, 0751 U.T. (figure 10*a*, Helliwell 1969).

FIGURE 6. Two representative examples of chorus observed near the dipole equator. The magnetometer lines at $\frac{1}{4}f_H$ and harmonics are indicated on the left. The top panel (df = 25 Hz, dt = 40 ms) shows chorus activity which may be divided into at least two distinct bands: one at and above one-half the electron gyrofrequency ($\frac{1}{2}f_H$); and the other somewhat below $\frac{1}{2}f_H$. The chorus emissions are rather poorly defined, and merge into hiss. The lower panel (df = 6.25 Hz, dt = 160 ms) shows two distinct bands of chorus activity. No discrete emissions or hiss were seen below the lower frequency limit of 1 kHz shown on the spectrogram. Most of the emissions are falling tones in both bands, but there seems to be very little correlation of emissions between the bands; thus the gap between the bands does not appear to be due simply to attenuation (figure 6, Burtis 1974).

FIGURE 7. Triggered emissions: artificially stimulated emissions (a.s.es) from the Morse-code dashes transmitted by station NAA; lines connect the direct wave observed near the transmitter with its whistler-mode echo observed near the conjugate point (figure 10*b*, Helliwell (1969)).

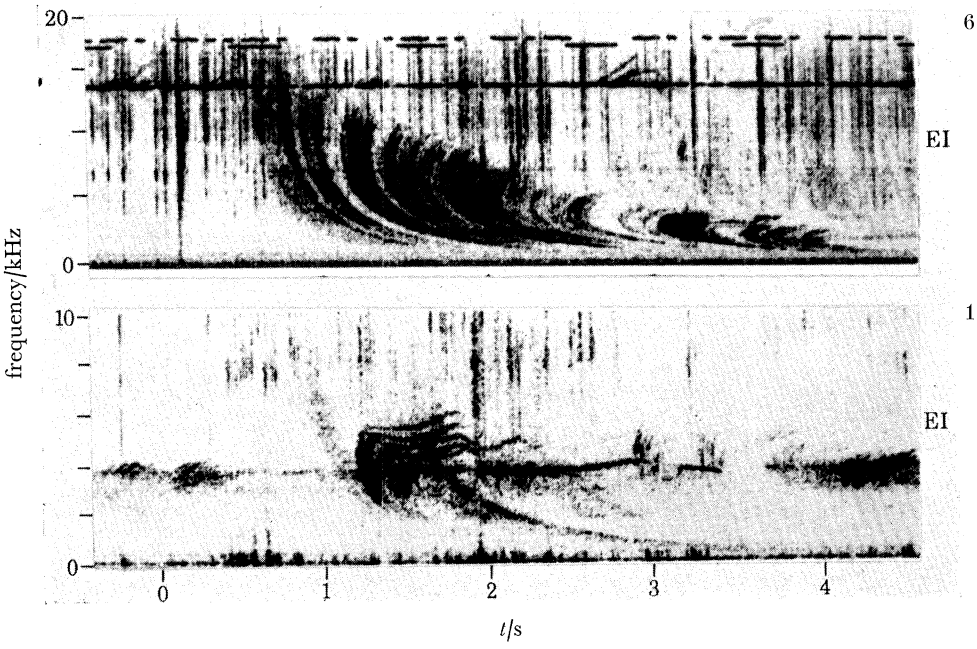

FIGURE 4. For description see opposite.

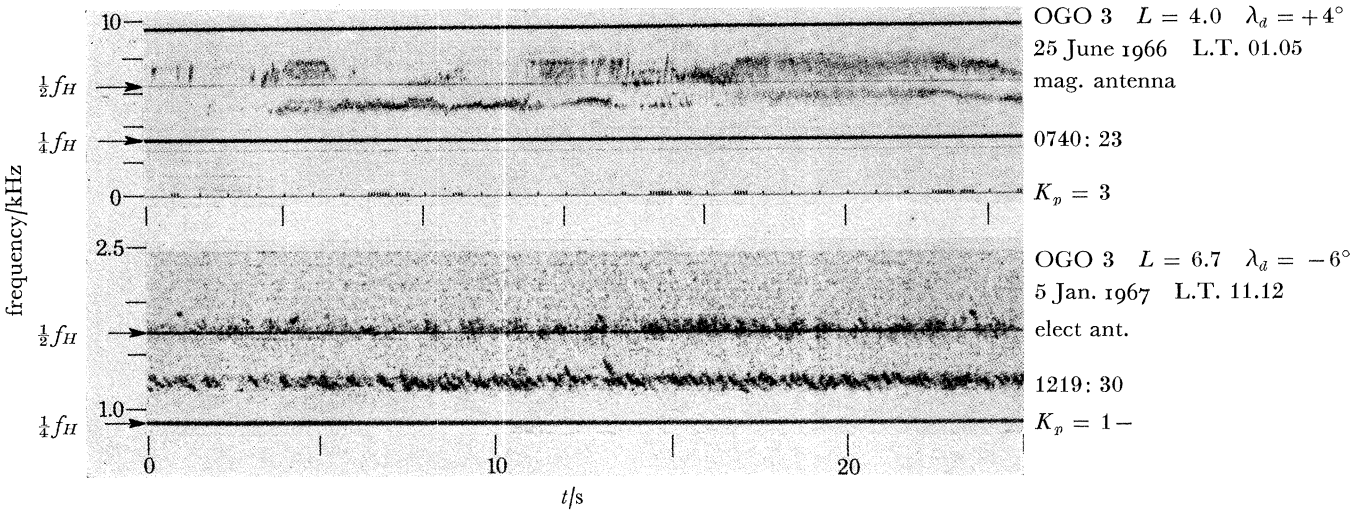

FIGURE 6. For description see opposite.

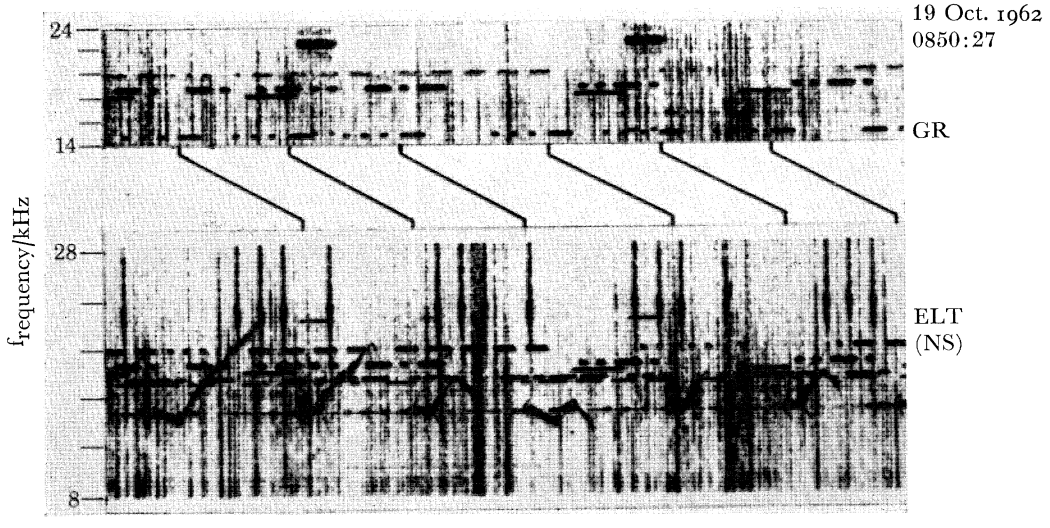

FIGURE 7. For description see opposite.

(*Facing p.* 140)

PHILOSOPHICAL TRANSACTIONS OF THE ROYAL SOCIETY A MATHEMATICAL, PHYSICAL & ENGINEERING SCIENCES

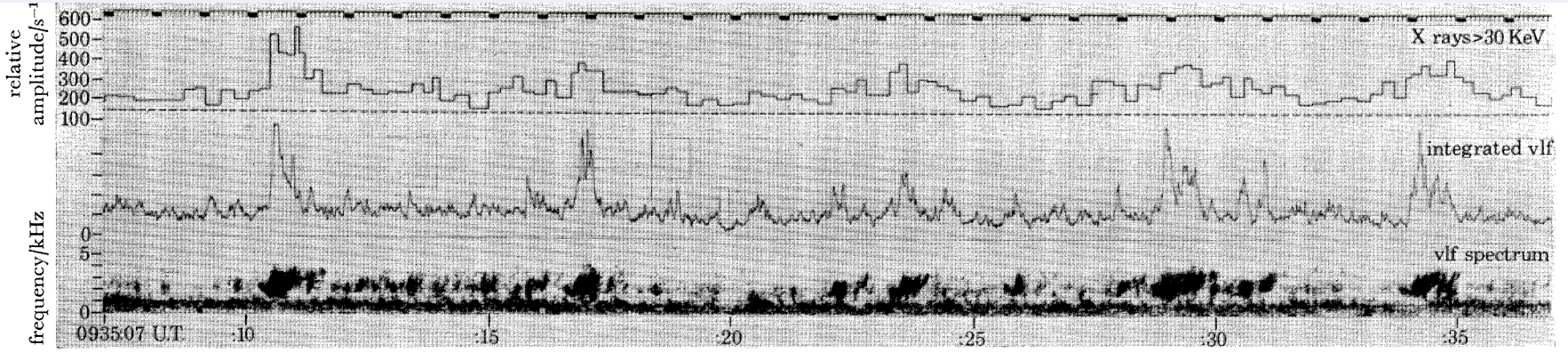

FIGURE 8. A 30 s segment of simultaneous recordings of X-ray count rate for $E > 30$ keV (top), integrated v.l.f. amplitude from 0.6 to 5 kHz (middle), and v.l.f. spectrum from 0 to 5 kHz (bottom), at Siple Station, Antarctica, on 2 January 1971. The dashed line in the top portion of the figure refers to the cosmic-ray background level of *ca.* 175 c/s. (Because of a plotting error the X-ray record must be shifted 0.15 s to the right relative to the v.l.f. records.) (figure 1, Rosenberg *et al.* (1971)).

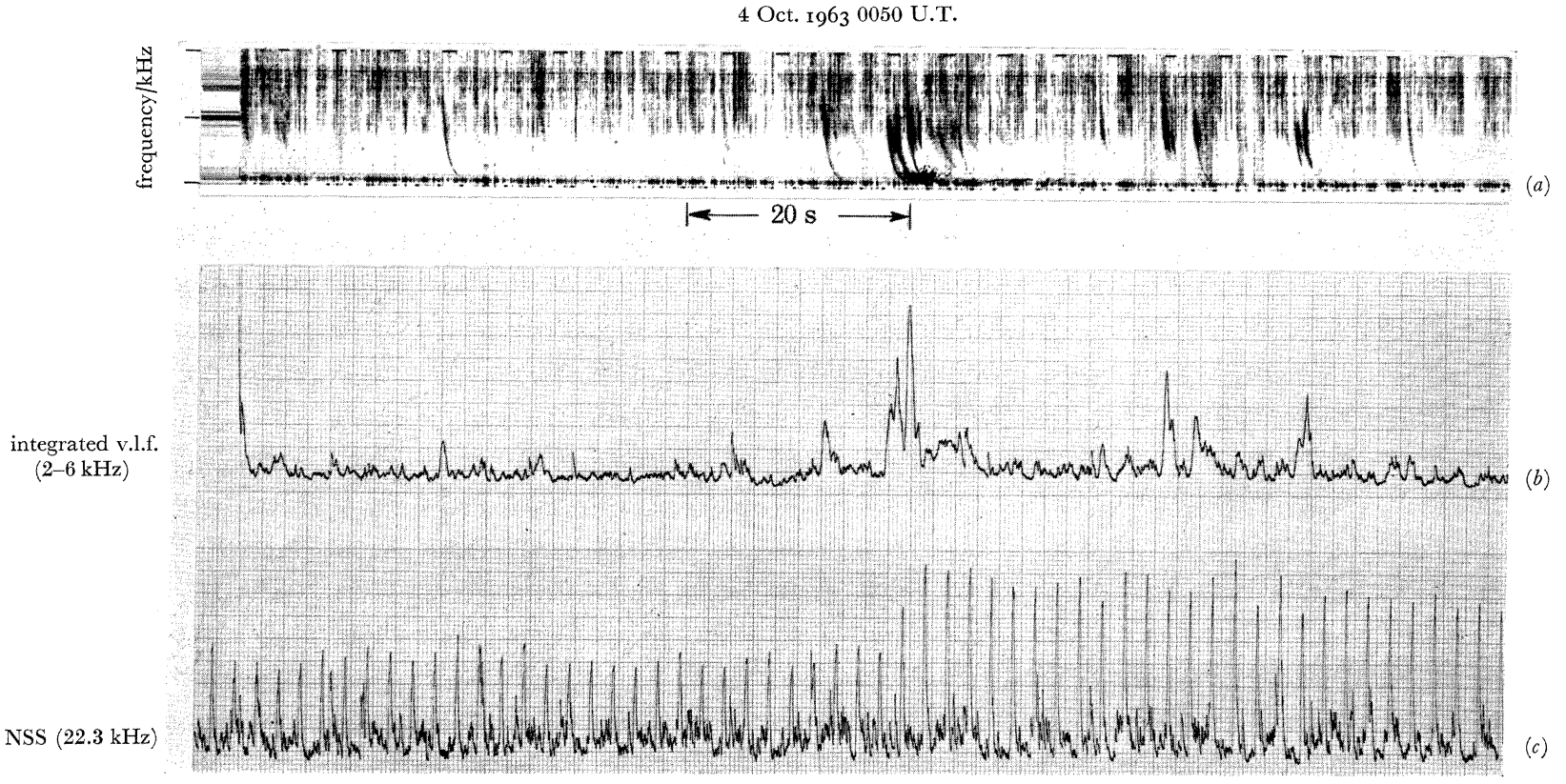

FIGURE 9. (*a*) Whistler spectra; (*b*) whistler amplitude, 2–6 kHz; and (*c*) NAA pulse transmissions, observed at Eights Station, Antarctica (figure 2, Helliwell, Katsufrakis & Trimpi (1973)).

types of 'ion' whistlers are observed including the subprotonospheric whistler (Barrington & Belrose 1963; Smith 1964) and the ion cutoff whistler (Muzzio 1968). Measurements of ion species and concentrations can thus be performed by using nonducted whistlers observed with satellites or rockets. Whistlers provide convenient remote sensing tools for study of the ionosphere and magnetosphere.

Other magnetospheric v.l.f. wave phenomena connected with whistlers are not so easily explained. In figure 4 for example the upper part shows emissions triggered by station NAA at 14.7 kHz. In the lower part a narrow-band emission is triggered at the upper cutoff frequency of each of several nose whistlers. An interesting class of emissions is the so-called non-dispersive periodic type. Each of its elements is triggered by the whistler-mode echo of the previous emission (Helliwell 1965). Sometimes groups of periodic emissions are observed to gradually rise in frequency in a quasi-periodic manner and to interact with whistlers (Ho 1973).

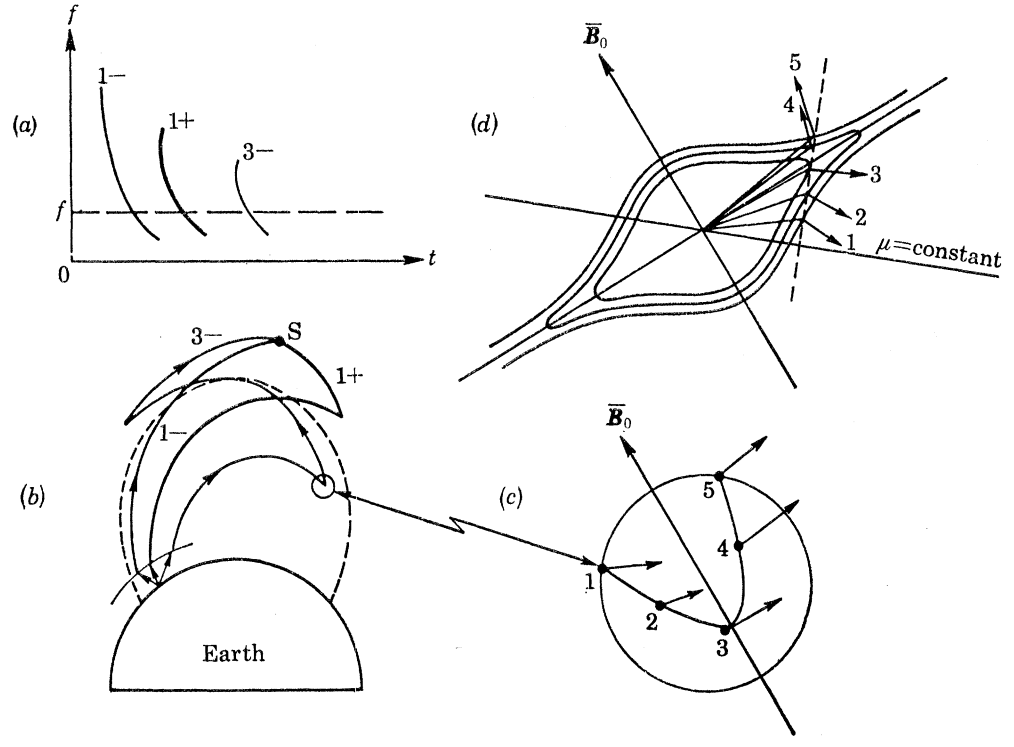

FIGURE 5. Interpretation of MR whistlers: (*a*) idealized spectrum observed in satellite; (*b*) ray paths to satellites at frequency *f*; (*c*) enlarged view of 'turn-around' region, showing wave normal directions; (*d*) refractive index surfaces in vicinity of 'turn-around', showing mechanism of reflexion. Dashed line is perpendicular to surfaces of constant refractive index (figure 6, Helliwell 1969).

In addition to the triggered emissions so common in ground data, there are many apparently spontaneous emissions both in ground data and in satellite data. In fact satellites located near the equatorial plane outside the plasmapause seldom see any whistler-mode signals other than spontaneous emissions. Examples of spontaneous banded chorus are shown in figure 6, plate 3 (Burtis 1974). Each record shows two well defined bands, although in many other cases only a single band is present. Measurements made over most of the magnetosphere show that virtually all chorus is banded and that the average frequency of the band bears a simple relation to the equatorial gyrofrequency along the line of force passing through the satellite. Analysis of this

relation provides strong evidence that the source of generation must lie close to the equator. The upper band of chorus, usually near half the equatorial gyrofrequency, is attributed to enhanced feedback in the oscillator that generates the chorus. The lower band may be controlled by the flux of resonant electrons. The reduced occurrence of chorus between these two bands is attributed to wave interference between two generated wave components having slightly different phase velocities (Burtis 1974). Spontaneous emissions show exponential growth rates, bandwidths and time rates of change of frequency similar to triggered emissions. However the growth rates of spontaneous emissions are larger, perhaps by a factor of 10, than those of triggered emissions.

Since lightning-excited natural whistlers frequently trigger emissions, we might expect man-made v.l.f. signals to do likewise. An example is shown in figure 7, plate 3. Each of the morse dashes, 150 ms duration, triggers a strong emission. Each triggered emission first rises in frequency and then may continue to rise or may fall in frequency. The intensities of these emissions usually exceed the intensity of the triggering signal. A curious feature of these results is the absence of triggering by the Morse dots, which are of 50 ms duration. The dot–dash anomaly will be discussed in more detail later.

Having reviewed briefly the properties of whistlers and emissions we now consider their effect on particle precipitation. These waves alter the pitch angles of resonant electrons, causing some to be precipitated into the ionosphere. One result of such precipitation is the production of Bremsstrahlung X-rays. An example of the association of > 30 keV X-ray bursts and v.l.f. emission bursts is shown in figure 8, plate 4 (Rosenberg, Helliwell & Katsufrakis 1971). Each emission is accompanied by a burst in the X-ray count.

Another association between v.l.f. waves and precipitation is illustrated in figure 9, plate 4. Each strong whistler causes a marked perturbation in the intensity of a v.l.f. signal propagating in the Earth–ionosphere waveguide. The changes in field intensity may be as large as 6 dB and can be negative as well as positive. The duration of the perturbation in field intensity is of the order of 30 s and is attributed to a temporary enhancement of electron density in the night-time D region. A mechanism to explain the wave-induced precipitation effects can be understood by reference to figure 2. It is supposed that the electrons to be precipitated resonate strongly with the waves near the equatorial plane. The wave fields scatter some electrons into the loss cone of the hemisphere from which the waves come. Some of these electrons in turn can be scattered back into the opposite hemisphere. These initially surprising results are in agreement with other evidence that much of the ionization in the night-time lower ionosphere can be attributed to precipitation of particles from the magnetosphere (Potemra & Zmuda 1970). Other evidence of wave-induced precipitation is found in connexion with the so-called 'slot' in the radiation belt intensity (Lyons & Thorne 1970). The search for such effects and their quantitative understanding is one of the objectives of the forthcoming International Magnetospheric Study (I.M.S.).

3. Model of electron wave interaction

The properties of natural and artificially stimulated narrowband emissions from the magnetosphere are not explainable by known theories of plasma instability. Especially puzzling is the dot–dash anomaly which suggests that a waiting time is required before the emission takes place. Using the observational facts, an attempt has been made to develop a new model of the interaction process. The starting point is the well known doppler-shifted cyclotron resonant interaction

between energetic electrons and whistler-mode waves. The model is illustrated in figure 10. Although cyclotron resonance is relatively easy to visualize and to apply, it cannot by itself explain the long enduring nature of some v.l.f. emissions and the high intensity which was noted in connexion with figure 1. Some coherent self-sustaining process is required which goes beyond known theories.

The suggestion has been made that the cyclotron-resonant electrons are phase bunched by a coherent wave travelling in the opposite direction (Brice 1963). The phase bunched electrons form transverse currents that are proportional to the perpendicular velocity $v_\perp$ of the electrons. These currents then radiate like circularly-polarized antennas, thus enhancing the fields which are required for the bunching. If the stimulated radiation is of sufficient intensity then this process becomes self sustaining. In essence each resonant electron must see resonant wave fields over a path that is many wavelengths long. Where the rate of change of doppler-shifted wave frequency is equal to the rate of change of the electron's gyrofrequency the length of such a resonance region has its maximum value. It is then easy to derive a relationship between the time rate of change of frequency and the location of the interaction region (Helliwell 1967, 1970). This relation provides a natural explanation for the rising and falling tones observed in the magnetosphere.

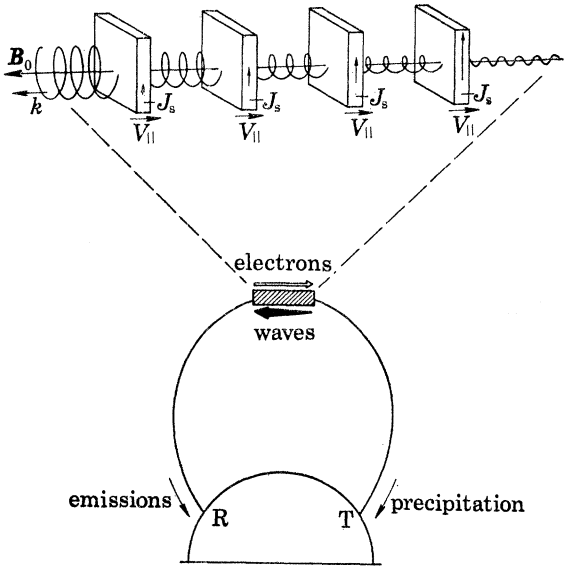

FIGURE 10. Sketch of interaction region, or emission cell, model. Circularly polarized waves transmitted from T resonate with oppositely travelling electrons near the equator. The train of electron sheets represents a continuous stream of resonant electrons. The resonant electrons in each sheet are phase-bunched by the wave, producing a transverse stimulated current J_s. The change in wave amplitude shown across each sheet results from the addition of the wave component generated by J_s. Emissions travel to R, and the scattered electrons are precipitated at T (figure 1, Helliwell & Crystal 1973).

Application of the model of figure 10 to a homogeneous region gives some interesting results relating the bunching process to the generation of the waves. It is supposed that the energetic electron population can be represented by sheets of electrons having uniformly distributed phases with respect to the $\boldsymbol{B}$ field of the wave. There is a sheet for each combination of pitch angle and parallel velocity near resonance. As each sheet moves through the wave the $q\boldsymbol{v}_\perp \times \boldsymbol{B}$ force alters the phase of each electron relative to the local B field of the wave, forming a temporary helical array that radiates in the direction of wave propagation. New particles continually

enter the region supplying energy in essentially a steady-state fashion. It is thus possible to construct a steady-state oscillator in which the phase-bunched electrons radiate the fields required to produce the phase-bunching. The energy for wave growth comes from the kinetic energy of the resonant electrons. The distribution of the wave magnetic field intensity and the perpendicular current density caused by phase bunching in a particular computer-simulated model are shown in figure 11 (Helliwell & Crystal 1973). In this model the theoretical bandwidth is zero because the process is in steady-state. On the other hand a small spread of electron parallel velocities and a wide spread of pitch angles is involved.

Analysis of this model has shown that the first order interaction process represented by figure 11 is independent of the time rate of change of frequency (Helliwell 1970). In addition the model predicts that rising tones will be observed only on the downstream (for the electrons) side of the

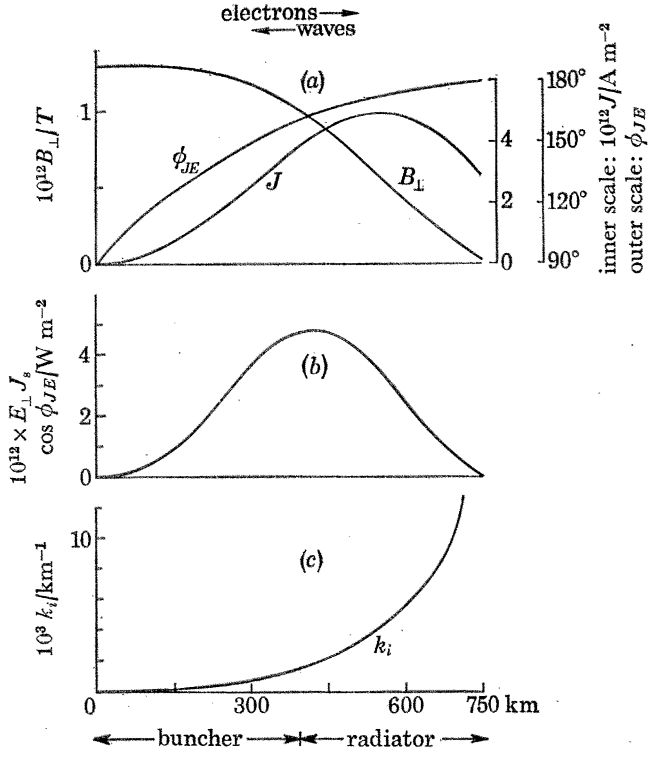

FIGURE 11. Interaction region cross section during self-sustained emission. (*a*) Steady state spatial variations of $B_\perp$, J_s, and ϕ_{JE} for self-excited oscillations, where $N_E = 2.8\ \mathrm{m^{-3}}$. (*b*) Power density generated by phase-bunched electrons. (*c*) Spatial growth rate k_i (figure 9, Helliwell & Crystal (1973)).

equator and falling tones only on the upstream side of the equator. Thus a satellite should not encounter falling tones on the equator. A recent experimental study of v.l.f. chorus made on the OGO 3 satellite has given support to this theoretical prediction (Burtis 1974). An important feature of the model whose steady-state behaviour is shown in figure 11, is the initial growth. The computer simulation shows that the oscillation grows exponentially in time when the triggering signal is much weaker than the saturation level of the oscillation. The result requires that the density of the energetic electrons in the resonant stream exceed a certain threshold value. The oscillation continues to grow in amplitude until it reaches saturation, after which it may fluctuate a little before it settles down to a constant-amplitude output.

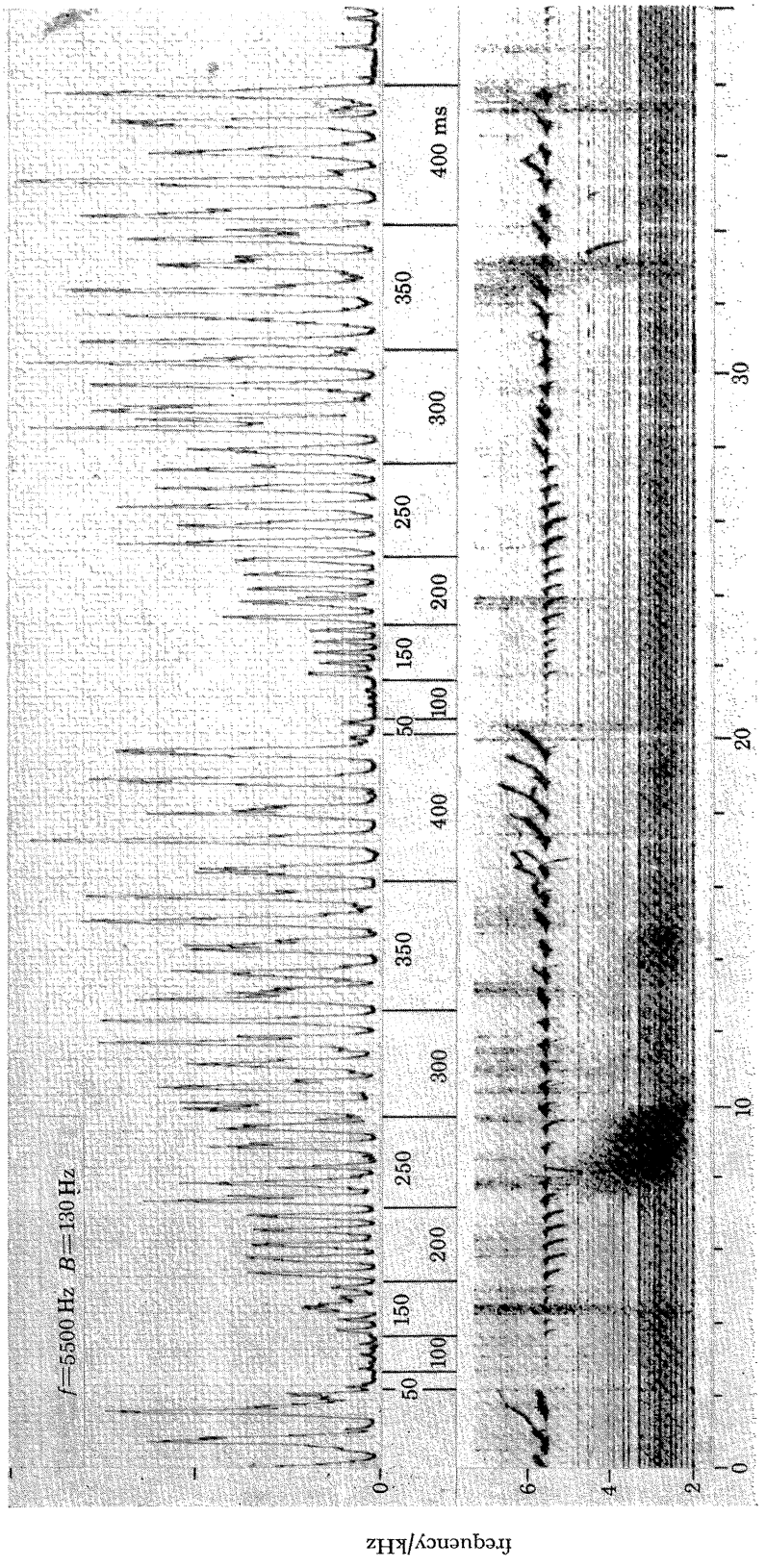

FIGURE 13. Variable pulse length sequence received at Roberval. Lower panel shows the spectrum, and upper panel shows the amplitude in a 130 Hz bandwidth centred on 5.5 kHz. Pulse lengths vary from 50 to 400 ms in 50 ms steps as indicated by the numbers between panels. A two-hop whistler, with echoes at *ca.* 3 kHz, appears at 8–10 s; its source is the sferic at 4.2 s. A strong well defined two-hop whistler component extending up to 5.5 kHz is seen at about 8.2 s and corresponds to the one-hop delay of the Siple pulses (figure 2, Helliwell & Katsufrakis (1974)).

(*Facing p.* 144)

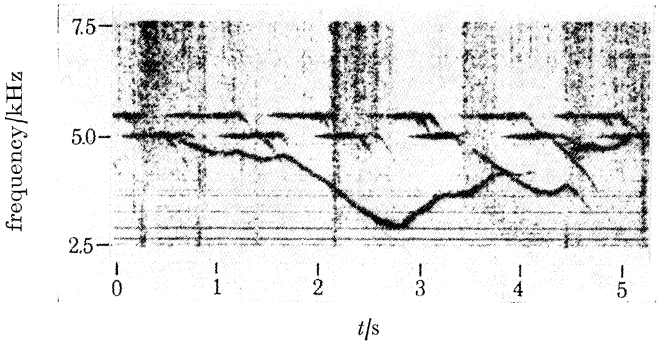

FIGURE 14. Hooks triggered at 5.0 kHz show inflexions and reversals in slope at power line harmonics, defined by the horizontal lines (figure 6, Helliwell & Katsufrakis (1974)).

PHILOSOPHICAL TRANSACTIONS OF THE ROYAL SOCIETY A MATHEMATICAL, PHYSICAL & ENGINEERING SCIENCES

4. Controlled wave injection experiments

In order to test the predictions of the theory outlined above and to extend the description of the experimental results, an experiment was designed as sketched in figure 12. A transmitting site was first established at Siple Station, Antarctica. The reasons for choosing such a remote location are important. First, it was necessary that the antenna be reasonably efficient. At these frequencies (down to 1 kHz) vertical antennas are either impractical or very expensive. Practical horizontal antennas radiate very little power over ordinary ground. However a thick ice sheet provides a relatively low-loss dielectric support which greatly increases the efficiency of the antenna. For example at 6 kHz the efficiency of the Siple antenna (23 km long and 5 m high)

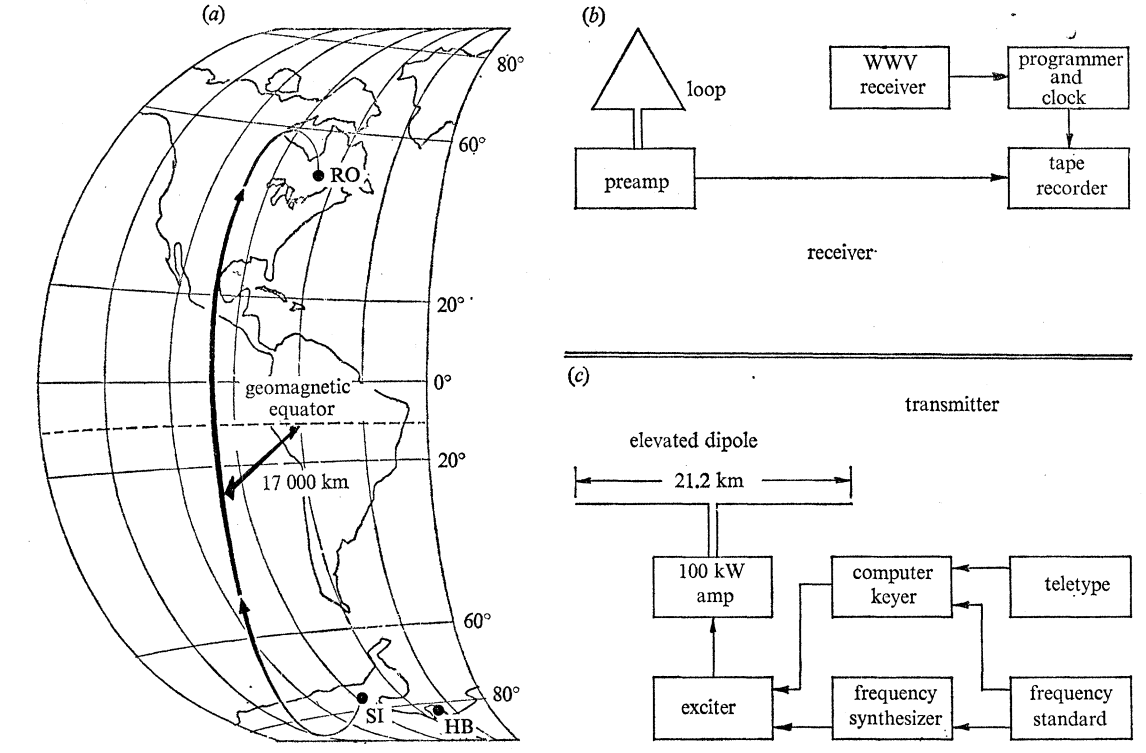

Figure 12. (*a*) Sketch of magnetospheric path from Siple Station (SI), Antarctica, to Roberval, Quebec (RO); 'HB' is Halley Bay. (*b*) Roberval v.l.f. receiver block diagram. (*c*) Siple v.l.f. transmitter block diagram (figure 1, Helliwell & Katsufrakis (1974)).

is estimated to be 4%. Another factor is the desirability of a location close to the plasmapause and to regions where the natural whistler and emission activity is high. Finally, it was necessary to locate the transmitter so that the conjugate point (near Roberval, Quebec) would be readily accessible. In addition to the receiver at Roberval, various satellites, such as Explorer 45, are employed in the observation of the magnetospheric signal excited by the transmitter. To date successful experiments have been conducted at frequencies from 1.95 up to 7.6 kHz.

One of the first experiments was a study of the effect of varying the pulse length, aimed at understanding the dot–dash anomaly. Some typical results are shown in figure 13, plate 5. Pulses ranging in duration from 50 to 400 ms were transmitted in groups of five with a 50 ms step in pulse length from one group to the next. The pulses were transmitted alternately on two

frequencies, 5.0 and 5.5 kHz. However, only the output on the upper frequency was strong at that particular time. The recordings show growth at the carrier frequency and subsequent triggering of emissions, both falling and rising. The dot–dash anomaly mentioned above is well defined in these records. The 50 ms pulses produce no detectable output whereas pulses exceeding 150 ms in duation are clearly visible. Both pulse intensity and triggered emission activity increase with pulse length.

A new fact uncovered by these particular tests was the observation that wave growth stops at or shortly after the termination of the triggering signal. For the shorter pulses, 100, 150 and 200 ms, an emission is excited which first rises slightly in frequency and then falls. As the pulse length increases the peak intensity of the output increases as shown in the amplitude chart in the upper part of figure 13. A detailed examination of individual pulses shows that for pulses of 250 ms duration or less the intensity grows exponentially with time. In figure 13, the total growth is about 30 dB for the longer pulses and the growth rate averages 128 dB/s.

Following saturation at the carrier frequency or termination of the triggering pulse, which ever occurs first, the frequency shifts upward and then may continue to rise as shown in the later parts of figure 13. If the triggering pulse terminates before the emission moves off frequency then a falling tone is often produced. The experiments have shown that a triggered emission will usually not cross another signal on the same path. Thus if the triggering signal remains 'on' when the triggered emission has been excited then the emission will continue rising in frequency or terminate rather than cross the exciting wave.

In view of the results shown in figure 13 the dot–dash anomaly of the earlier observations is easily understood. Exponential growth occurs most often when a coherent triggering signal is present. When that signal terminates the growth may or may not continue for a short time, but in any case the emission soon decays back to the noise level. Thus a 50 ms pulse is not long enough to produce significant growth and hence no emissions are observed.

Other types of response have been observed including multipath propagation with strong growth on each path. In such cases emission traces may cross one another on the record. However it has been found that the crossing traces are on different magnetospheric paths.

A new type of wave–wave interaction has been discovered in these experiments and is illustrated in figure 14, plate 6. Here the triggered emission reverses its slope at the frequency of a Roberval power line harmonic. In addition as it rises in frequency the emission is observed to dwell on another power line component. Interaction between triggered emissions and power line harmonics occurs frequently. The interaction may take the form of a change in slope as shown in figure 14 or a cutoff of the emission. In some cases the emission will cut off at one power line harmonic and turn on at another.

To demonstrate the existence in the magnetosphere of radiation associated with power lines, conjugate recordings were made at Siple Station, Antarctica and Roberval, Quebec (Helliwell, Katsufrakis, Bell & Raghuram 1975). It was found that conjugate line radiation could be observed with identical frequencies but with intensity modulation that was 180° out of phase at the two ends of the path. This result is in accord with the whistler echo pattern illustrated in figure 2. The lines were spaced about 120 Hz apart, a strong indication of power line association.

In the course of these experiments it was discovered that the actual magnetospheric line radiation was not exactly at the frequency of the original power line frequency. Instead it was often higher by 20 or 30 Hz. A possible explanation was triggering first by the harmonic itself and then triggering by the echo of the earlier emission. Such a mechanism is in accord with

PHILOSOPHICAL TRANSACTIONS OF THE ROYAL SOCIETY A MATHEMATICAL, PHYSICAL & ENGINEERING SCIENCES

figure 13 in which most emissions triggered by the longer pulses rise in frequency. However, in some cases the line radiation was slightly below the nearest power line harmonic.

It was concluded that the power line radiation arises from the large harmonic content, long lines and heavy loads of the Canadian power system. The Siple Station experiments have indicated that excitation of emissions can occur for radiated powers of less than 10 W. Thus it is plausible to ascribe the observed spectral lines to actual radiation from the power system. It seems likely that other power systems of the World may also exercise similar control of the magnetosphere through excitation of whistler-mode signals.

Another interesting effect of the exciting signals (both from Siple Station and from power lines) is the creation of a band of reduced noise just below the frequency of the transmitter. Varying in width from 50 to 200 Hz this band appears to result from a reduction in the background hiss coming out of the magnetosphere. Apparently the triggering signal is able to suppress the growth of natural noise in this narrow band. The band usually takes several seconds to develop, and may last even longer after the exciting signal is terminated. It might play a useful role in improving the signal-to-noise ratio on a v.l.f. channel in which the noise arises in the magnetosphere.

5. Conclusions

Predictions of the model described here and experimental observations of spontaneous and triggered emissions appear to be converging. The new wave injection experiments show promise of answering many of the remaining questions regarding the properties of v.l.f. emissions. When a full theory is available it may be possible to use stimulated emissions to measure the properties of trapped energetic electrons in the magentosphere. Thus v.l.f. waves in the magnetosphere could play a dual role as diagnostic tools for both the hot and cold components of the magnetospheric plasma. Much of this work can be carried out on the ground, thereby reducing the need for satellites.

V.l.f. waves cause precipitation of energetic particles into the ionosphere. By controlling this precipitation flux through v.l.f. wave-injection new kinds of experiments on the ionosphere may be possible. Since the energy of the precipitated particles depends on wave frequency it should be possible to control the height of deposition of the precipitated energy. The response of the ionosphere to such excitation could be studied by using a variety of instruments, including X-ray detectors, v.l.f. receivers (for both phase and intensity), riometers, ionosondes, photometers, magnetometers, and incoherent scatter radars. Modification of the propagation characteristics of the ionosphere with the aid of v.l.f. waves is now possible.

Control of the wave-particle interaction process in the magnetosphere can lead to new types of plasma physics experiments which require a large volume of plasma. Since wave-particle interactions are characteristic of all plasmas, such experiments should be of interest to laboratory plasma physics and to astrophysics as well as to magnetospheric physics. Spontaneous emissions and artifically triggered emissions are much alike. Therefore it follows that the fundamentals of this apparently ubiquitous natural process are now accessible to controlled experimentation. A practical form of such an experiment at present would be to inject waves from the ground and to observe the wave growth and associated particle distribution function in a satellite situated in the interaction region. Later it may be possible to simultaneously inject waves and energetic particles from a satellite.

New techniques of communication might be based on the observed wave-particle interactions

PHILOSOPHICAL TRANSACTIONS OF THE ROYAL SOCIETY A MATHEMATICAL, PHYSICAL & ENGINEERING SCIENCES

in the magnetosphere. With a magnetospheric gain of 30 dB, on 1 kW transmitter becomes equivalent to a 1 MW transmitter in the absence of gain. Further improvements in signal/noise ratio might be achieved through wave-induced narrow spectral bands of reduced noise.

References (Helliwell)

Angerami, J. J. 1970 Whistler duct properties deduced from v.l.f. observations made with the OGO 3 satellite near the magnetic equator. *J. geophys. Res.* **75**, 6115–6135.

Barkhausen, H. 1919 Zwei mit Hilfe der neuen Verstärker entdeckte Erscheinungen. *Physik. Z.* **20**, 401–403.

Barrington, R. E. & Belrose, J. S. 1963 Preliminary results from the very-low-frequency receiver aboard Canada's Alouette satellite. *Nature, Lond.* **198**, 651–656.

Barrington, R. E. & McEwen, D. J. 1966 *Space research*, VII, p. 624. Amsterdam: North Holland Publishing Co.

Brice, N. M. 1963 An explanation of triggered v.l.f. emissions. *J. geophys. Res.* **68**, 4626–4628.

Burtis, W. J. 1974 Magnetospheric chorus. Tech. Rept. No. 3469–3, Stanford University, Stanford, Calif., U.S.A.

Burton, E. T. & Boardman, E. M. 1933 Audio-frequency atmospherics. *Proc. I.R.E.* **21**, 1476–1494.

Carpenter, D. L., Stone, Keppler, Siren, Jan C. & Crystal, T. L. 1972 Magnetospheric electric fields deduced from drifting whistler paths. *J. geophys. Res.* **77**, 2819–2834.

Carpenter, D. L. & Park, C. G. 1973 On what ionospheric workers should know about the plasmapause–plasmasphere. *Rev. Geophys.* **11**, 133–154.

Dunckel, N. 1974 Low-frequency radio emissions from the Earth and Sun. Tech. Rept. No. 3469-2, Stanford University, Stanford, Calif., U.S.A.

Eckersley, T. L. 1935 Musical atmospherics. *Nature, Lond.* **135**, 104–105.

Gurnett, D. A., Shawhan, S. D., Smith R. L. & Brice, N. M. 1965 Ion cyclotron whistlers. *J. geophys. Res.* **70**, 1665–1688.

Helliwell, R. A. 1965 *Whistlers and related ionospheric phenomena.* Stanford, Calif., U.S.A.: Stanford University Press.

Helliwell, R. A. 1967 A theory of discrete v.l.f. emissions from the magnetosphere. *J. geophys. Res.* **72**, 4773–4790.

Helliwell, R. A. 1969 Low-frequency waves in the magnetosphere. *Rev. geophys.* **7**, 281–303.

Helliwell, R. A. 1970 Intensity of discrete v.l.f. emissions, *Particles and fields in the magnetosphere* (ed. B. M. McCormac) pp. 292–301.

Helliwell, R. A. & Crystal, T. L. 1973 A feedback model of cyclotron interaction between whistler-mode waves and energetic electrons in the magnetosphere. *J. geophys. Res.* **78**, 7357–7371.

Helliwell, R. A. & Katsufrakis, J. P. 1974 V.l.f. wave injection into the magnetosphere from Siple Station, Antarctica. *J. geophys. Res.* **79**, 2511–2518.

Helliwell, R. A., Katsufrakis, J. P. & Trimpi, M. L. 1973 Whistler-induced amplitude perturbation in v.l.f. propagation. *J. geophys. Res.* **78**, 4679–4688.

Helliwell, R. A., Katsufrakis, J. P., Bell, T. F. & Raghuram, R. 1975 V.l.f. line radiation in the Earth's magnetosphere and its association with power line radiation. *J. geophys. Res.* (submitted August 1974).

Ho, D. 1973 Interaction between whistlers and quasi-periodic v.l.f. emissions. *J. geophys. Res.* **78**, 7347–7356.

Lyons, L. R. & Thorne, R. M. 1970 The magnetospheric reflection of whistlers. *Planet. Space Sci.* **18**, 1753–1767.

Muzzio, J. L. R. 1968 Ion cutoff whistlers. *J. geophys. Res.* **73**, 7526–7529.

Park, C. G. 1972 Methods of determining electron concentrations in the magnetosphere from nose whistlers. Tech. Rept. No. 3454-1, Stanford University, Stanford, Calif., U.S.A.

Potemra, T. A. & Zmuda, A. J. 1970 Precipitating energetic electrons as an ionization source in the mid-latitude nightime D region. *J. geophys. Res.* **75**, 7161–7167.

Rosenberg, T. J., Helliwell, R. A. & Katsufrakis, J. P. 1971 Electron precipitation associated with discrete very-low-frequency emissions. *J. geophys. Res.* **76**, 8445–8452.

Smith, R. L. 1964 An explanation of subprotonospheric whistlers. *J. geophys. Res.* **69**, 5019–5022.

Smith, R. L., Helliwell, R. A. & Yabroff, I. W. 1960 A theory of trapping of whistlers in field-aligned columns of enhanced ionization. *J. geophys. Res.* **65**, 805–823.

Storey, L. R. O. 1953 An investigation of whistling atmospherics. *Phil. Trans. R. Soc. Lond.* A **246**, 113–141.

PHILOSOPHICAL TRANSACTIONS OF THE ROYAL SOCIETY A MATHEMATICAL, PHYSICAL & ENGINEERING SCIENCES

Discussion

K. Bullough (*Department of Physics, University of Sheffield*). Professor Helliwell has reported the identification of mains harmonics in v.l.f. emission data recorded at Siple. Morphological studies of v.l.f. emissions observed on Ariel 3 have shown that there is a strong maximum in the occurrence of v.l.f. emissions (2.7–3.7 kHz) centred on the U.S.A. In fact for this range of L shells ($2 < L < 4$) extending from lower Canada to the Mexican border the contribution from this longitude sector far exceeds that from any other part of the World. It seems probable that this may be due partly to the configuration of the geomagnetic field, America lying to the west of the South Atlantic anomaly and, partly, to the rich sources of man-made signals (mains harmonics) extending through the e.l.f. and low v.l.f. range of frequencies.

PHILOSOPHICAL TRANSACTIONS OF THE ROYAL SOCIETY A MATHEMATICAL, PHYSICAL & ENGINEERING SCIENCES

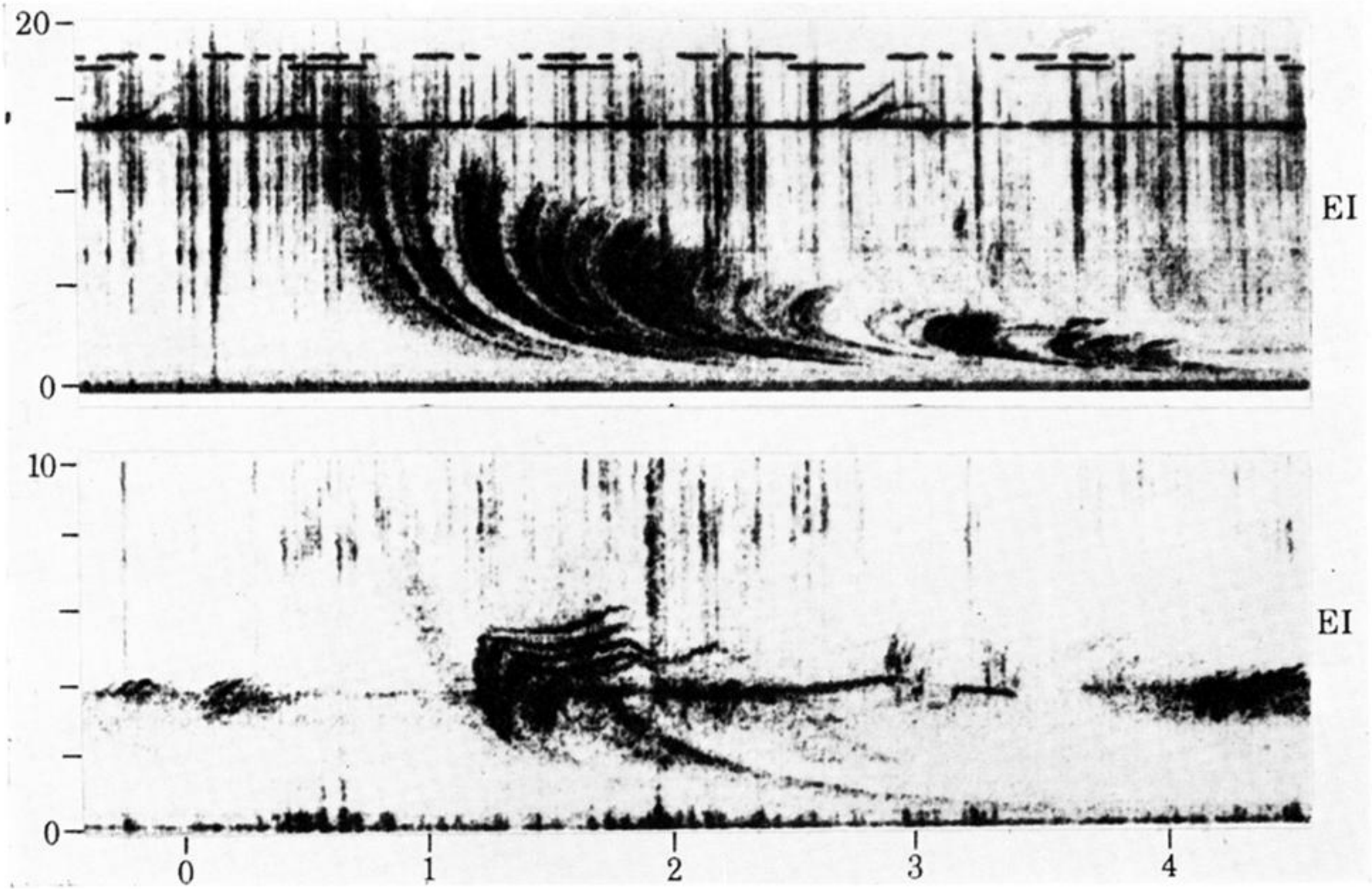

FIGURE 4. For description see opposite.

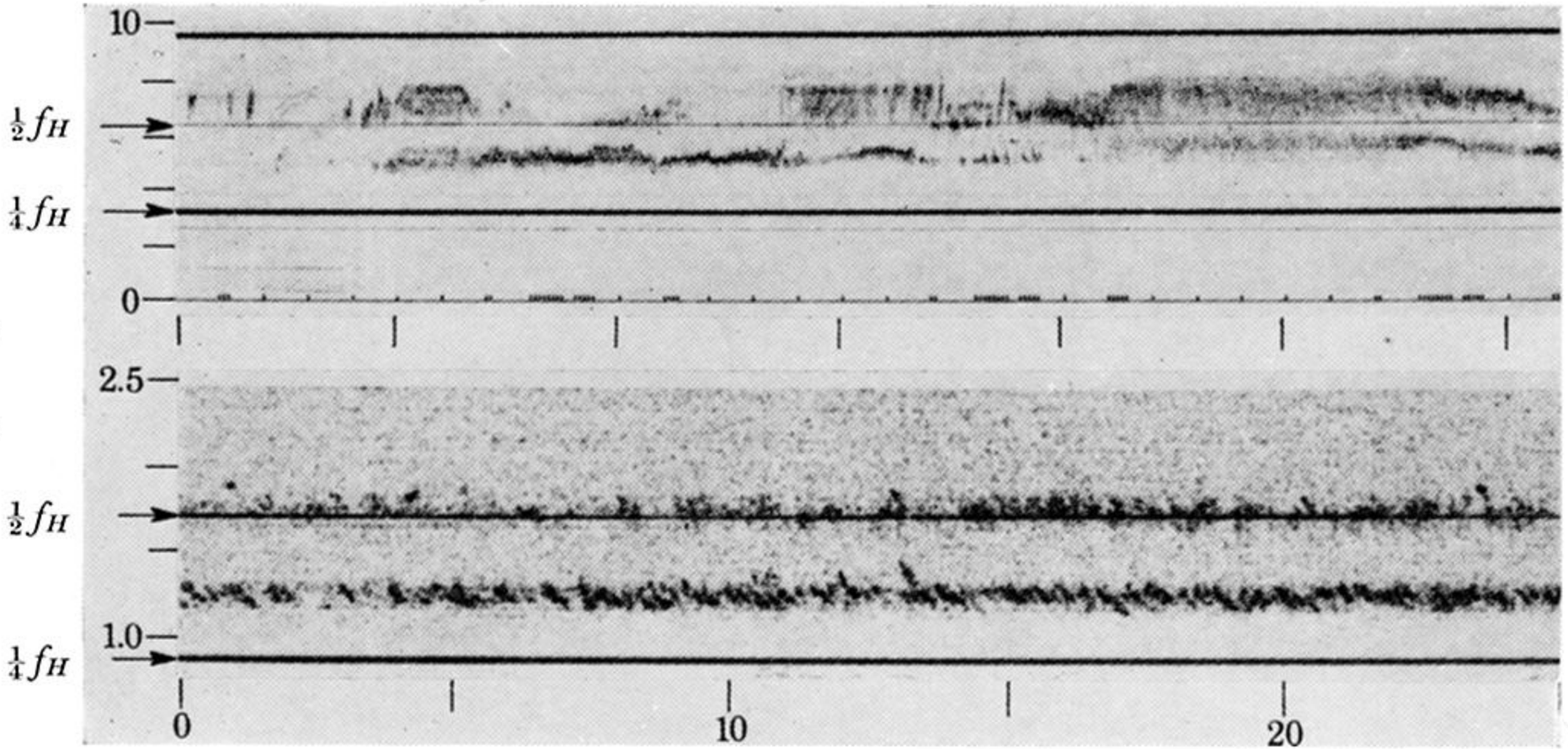

OGO 3 $L = 4.0$ $\lambda_d = +4°$
25 June 1966 L.T. 01.05
mag. antenna

0740: 23

$K_p = 3$

OGO 3 $L = 6.7$ $\lambda_d = -6°$
5 Jan. 1967 L.T. 11.12
elect ant.

1219: 30

$K_p = 1-$

FIGURE 6. For description see opposite.

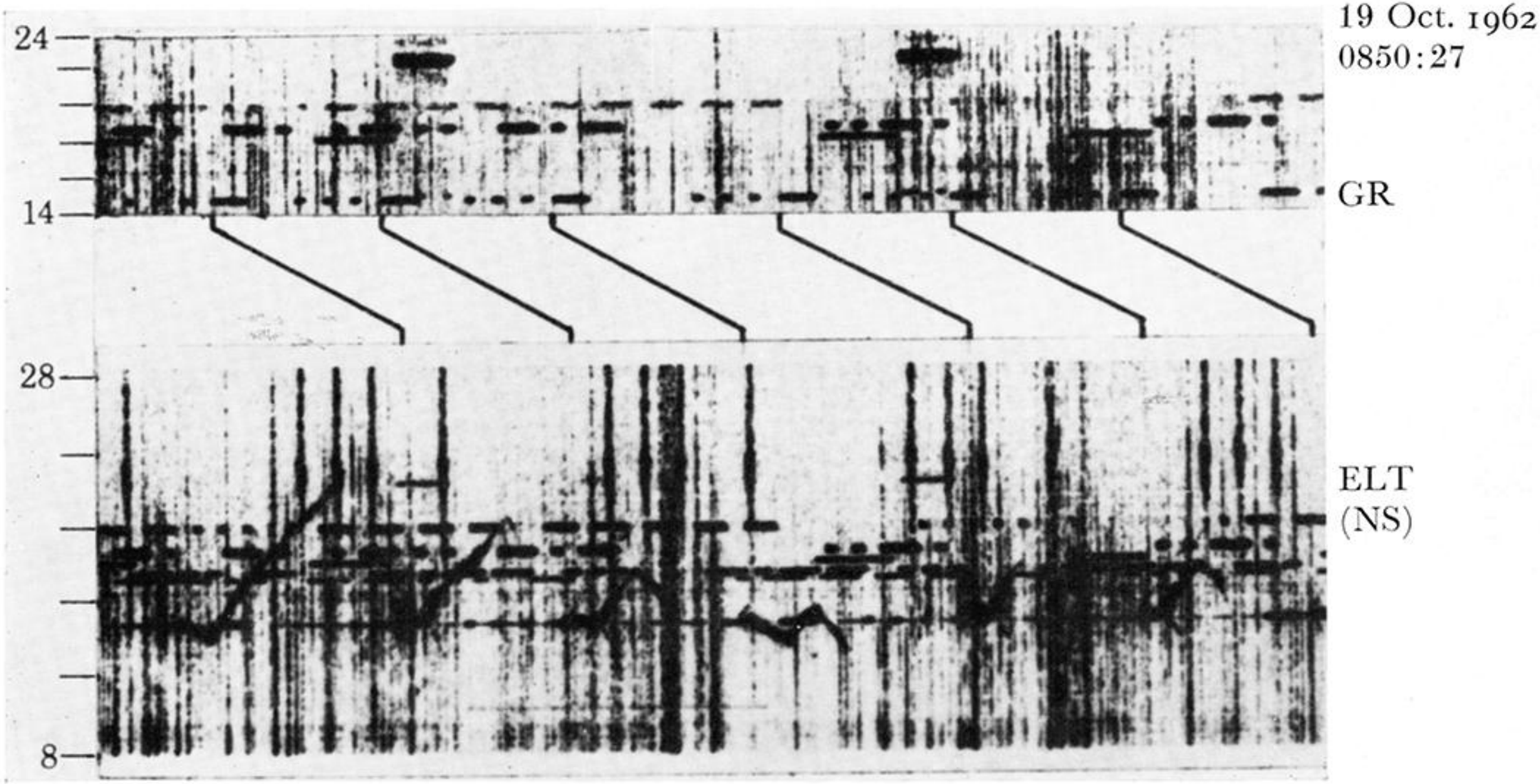

FIGURE 7. For description see opposite.

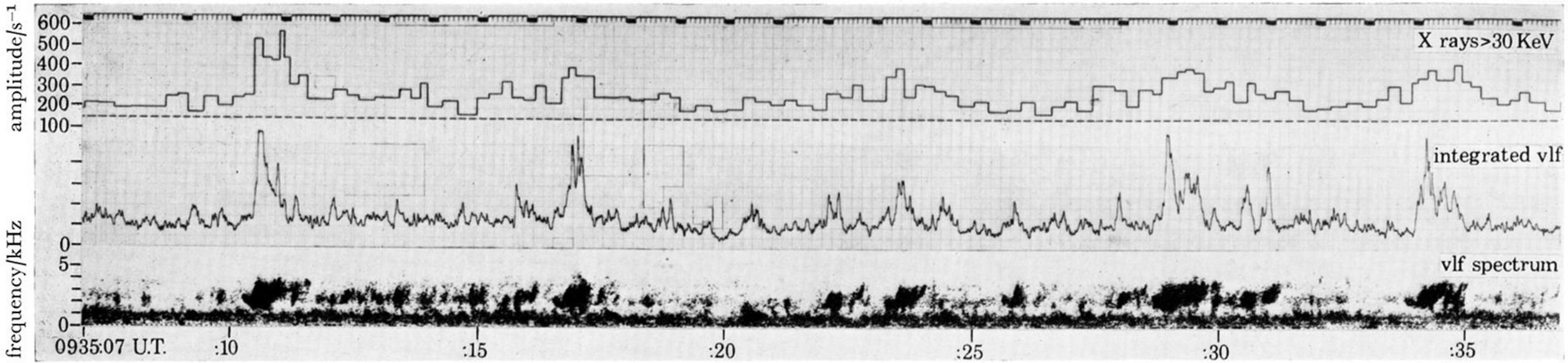

FIGURE 8. A 30 s segment of simultaneous recordings of X-ray count rate for $E > 30$ keV (top), integrated v.l.f. amplitude from 0.6 to 5 kHz (middle), and v.l.f. spectrum from 0 to 5 kHz (bottom), at Siple Station, Antarctica, on 2 January 1971. The dashed line in the top portion of the figure refers to the cosmic-ray background level of *ca.* 175 c/s. (Because of a plotting error the X-ray record must be shifted 0.15 s to the right relative to the v.l.f. records.) (figure 1, Rosenberg *et al.* (1971)).

FIGURE 9. (*a*) Whistler spectra; (*b*) whistler amplitude, 2–6 kHz; and (*c*) NAA pulse transmissions, observed at Eights Station, Antarctica (figure 2, Helliwell, Katsufrakis & Trimpi (1973)).

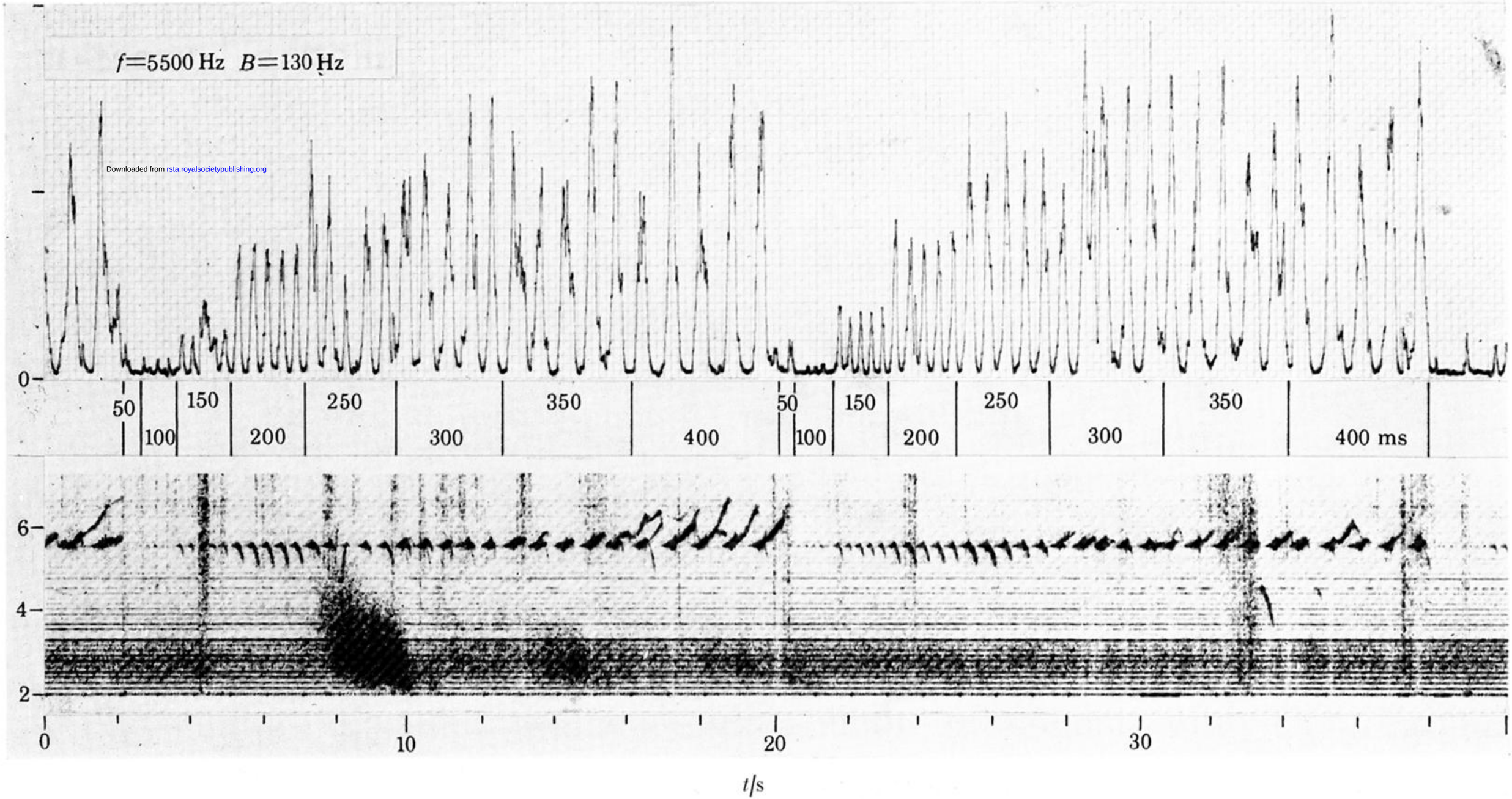

FIGURE 13. Variable pulse length sequence received at Roberval. Lower panel shows the spectrum, and upper panel shows the amplitude in a 130 Hz bandwidth centred on 5.5 kHz. Pulse lengths vary from 50 to 400 ms in 50 ms steps as indicated by the numbers between panels. A two-hop whistler, with echoes at *ca.* 3 kHz, appears at 8–10 s; its source is the sferic at 4.2 s. A strong well defined two-hop whistler component extending up to 5.5 kHz is seen at about 8.2 s and corresponds to the one-hop delay of the Siple pulses (figure 2, Helliwell & Katsufrakis (1974)).

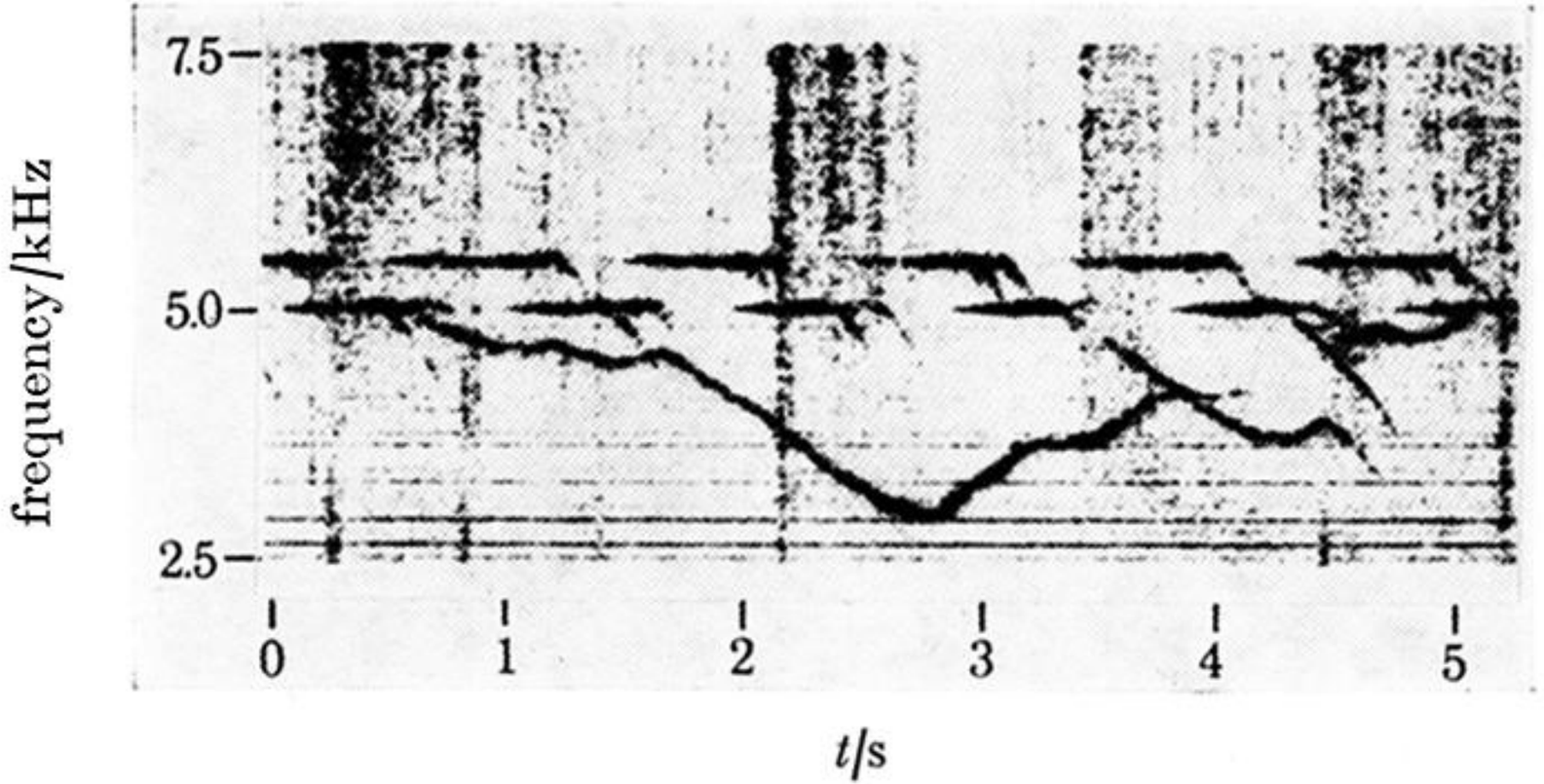

FIGURE 14. Hooks triggered at 5.0 kHz show inflexions and reversals in slope at power line harmonics, defined by the horizontal lines (figure 6, Helliwell & Katsufrakis (1974)).